Available online at www.sciencedirect.com
ScienceDirect
Renewable Energy 32 (2007) 1967–1980
RENEWABLE ENERGY
www.elsevier.com/locate/renene

Second law optimization of a solar air heater having chamfered rib–groove roughness on absorber plate

Apurba Layek[a,*], J.S. Saini[b], S.C. Solanki[b]

[a]Department of Mechanical Engineering, NIT Durgapur, Durgapur 713 209, India
[b]Department of Mechanical and Industrial Engineering, IIT Roorkee, Roorkee, Uttaranchal 247 667, India

Received 26 September 2006; accepted 17 November 2006
Available online 8 January 2007

Abstract

Artificially roughened solar air heaters perform better than the plane ones under the same operating conditions. However, artificial roughness leads to even more fluid pressure thereby increasing the pumping power. The entropy generation in the duct of solar air heater having repeated transverse chamfered rib–groove roughness on one broad wall is studied numerically. Roughness parameters, viz., relative roughness pitch P/e, relative roughness height e/D_h relative groove position g/P, chamfer angle ϕ and flow Reynolds number Re have a combined effect on the heat transfer as well as fluid friction. The entropy generation is minimized and reasonably optimized designs of roughness are found.

Keywords: Compound roughness; Solar air heater; Entropy generation

1. Introduction

Flat-plate solar collectors are extensively used in low temperature energy technology and have attracted the attention of a large number of investigators. Several designs of solar air heaters have been developed over the years in order to improve their performance. The thermal performance of a solar air heater is significantly low because of the low value of the convective heat transfer coefficient between the absorber plate and the air, leading to high absorber plate temperature and greater heat losses to the surroundings. It has been

*Corresponding author. Tel./fax: +91 1332 285665.
E-mail address: apurba_layek@yahoo.co.in (A. Layek).

0960-1481/$ - see front matter
doi:10.1016/j.renene.2006.11.005

Nomenclature

A_p	absorber plate area, m^2
C_p	specific heat of air, J/kg K
e	rib height (and groove depth), m
e/D_h	relative roughness height
f	friction factor
g	groove position, m
g/P	relative groove position
h	heat transfer coefficient, $W/m^2 K$
H	duct depth, m
k	thermal conductivity of air, W/m K
$\dot{m}$	mass flow rate, kg/s
P	rib pitch, m
P/e	relative roughness pitch
$\dot{S}_{gen}$	entropy generation rate, W/K
T_a	ambient temperature, °C
T_{fm}	bulk mean air temperature, °C
T_i	inlet air temperature, °C
T_o	outlet air temperature, °C
T_{pm}	mean plate temperature, °C
U_l	heat loss coefficient, $W/m^2 K$
W	duct width, m
δp	pressure drop in duct, Pa
ρ	density of air, kg/m^3
μ	dynamic viscosity, Pa s
ϕ	chamfer angle, degree
ψ	irreversibility distribution ratio

Subscript

s	smooth duct

found that the main thermal resistance to the heat transfer is due to the formation of a laminar sub-layer on the heat-transferring surface. Efforts of improving the heat transfer rate have been directed towards artificially destroying sub-layer. An artificial roughness on the heat transfer surface in the form of projections mainly creates turbulence near the wall, breaks the laminar sub-layer and thus enhances the heat transfer coefficient with a minimum pressure loss penalty. Artificial roughnesses of various geometrical shapes have been employed for the enhancement of the heat transfer coefficient from a surface [1–5] of different shapes. However this brings about a substantial increase in pumping power also. It is reported that the geometry of the roughness (roughness shape, pitch, height, etc.), has a marked influence on the heat transfer and friction characteristics of the surface. Ravigururajan and Bergles [3] used roughness in the form of semi-circular, circular, rectangular and triangular ribs to develop the general statistical correlations for heat transfer and pressure drop for single phase turbulent flow in internally ribbed surface. Liou and Hwang [2] tested the shapes of rib roughness in the form of square, triangular and semicircular cross section to study the effect of rib shapes on turbulent heat transfer and friction in a rectangular channel with two opposite ribbed walls, and reported that the square ribs give best heat transfer performance among them. Williams et al. [4] and Karwa et al. [1] have reported strong effect of chamfering of rib head on the heat transfer and friction characteristics. It is believed that chamfering of the rib reattaches the flow nearer the rib as well as frequent shedding of vortex at the rib top creates more turbulence and heat transfer. Zhang et al. [5] reported that the addition of grooves in between two square ribs creates an additional vortex within the groove which enhances the turbulence in the inter-rib zone as well as heat transfer with nearly same pressure drop. Simultaneously, groove creates the flow to reattach nearer to the rib decreases the reattachment length as well as the pitch length. It appears that it will be fruitful to investigate the performance of a solar air heater having absorber plate artificially roughened with optimally chamfered rib–groove roughness in order to achieve further enhancement of heat transfer rate.

As implied from the discussion of the effect of any augmentation technique improves the thermal contact will, most likely, cause a parallel increase in the mechanical power required to flow the air through the duct. Given this conflict, it is useful to know in advance which roughness parameters of an artificial roughness will lead to an improvement in the performance of solar air heater. In addition to that it is important to know in quantitative terms the magnitude of the improvement. The task of properly evaluating the merit of a proposed artificial roughness augmentation technique is, perhaps, as important as developing and applying the technique.

To the best of author's knowledge, the second law analysis of the solar air heater had rarely been reported. In the present study, the main concern is to develop a thermodynamic basis for evaluating the merit of augmentation technique of solar air hearer. It can be regarded that artificial roughness as design changes whose ultimate purpose is to inhibit the one-way destruction of exergy, thus paving the way toward thermodynamically efficient equipment.

In the present work, a methodology has been presented for thermodynamic optimization of a solar air heater having its absorber plate roughened with integral chamfered rib–groove roughness transverse to the flow of air as shown in Fig. 1. The numerical analysis has been carried out using the correlation of heat transfer coefficient and friction factor obtained from experimental investigation done by the authors (detailed experimentation, quantitative results and correlations are discussed in paper communicated to International journal of heat and mass transfer).

2. Mathematical modeling

Let us consider the system, similar to the heat transfer between the absorber plate and air flowing through the duct, in which two surfaces of different temperatures (T_{H} and T_{L}) experience the heat transfer interaction $\dot{Q}$, through the temperature gap. The second law states that the entropy generated by the system is finite as long as the temperature difference, $T_{\mathrm{H}} - T_{\mathrm{L}}$ is finite:

$$\dot{S}_{\mathrm{gen}} = \frac{\dot{Q}}{T_{\mathrm{L}}} - \frac{\dot{Q}}{T_{\mathrm{H}}} = \frac{\dot{Q}}{T_{\mathrm{L}}T_{\mathrm{H}}}(T_{\mathrm{H}} - T_{\mathrm{L}}) \geqslant 0. \tag{1}$$

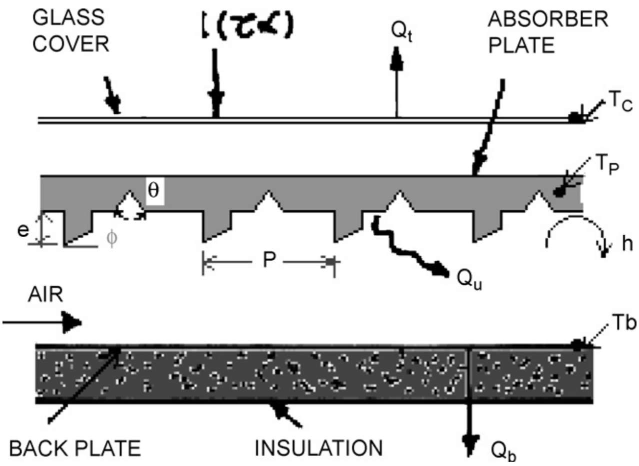

Fig. 1. Solar air heater with roughened absorber plate.

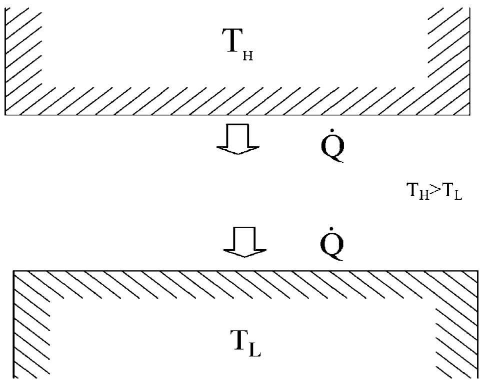

Fig. 2. Heat transfer across a non-zero temperature difference.

The true effect of a proposed augmentation technique on thermodynamic performance can be evaluated by comparing the irreversibility of the solar air heater duct before and after the implementation of the augmentation technique. Considering the general heat exchange passage referred in Fig. 2, any effort in reducing the temperature difference reduces the entropy generation rate (Eq. (1)). Let us consider the solar air heater flow passage of cross-section A and the heat transferring surface of width W shown schematically in Fig. 3. The bulk properties of the stream $\dot{m}$ (mass flow rate) are T_{f} (bulk fluid temperature), P (pressure), h (enthalpy), s (entropy) and ρ (density). In general, this heat transfer arrangement is characterized by a finite frictional pressure gradient $-\mathrm{d}P/\mathrm{d}x > 0$ and the heat transfer rate to the stream per unit length of the duct is q' (W/m) by a finite wall–bulk fluid temperature difference ΔT_{m}.

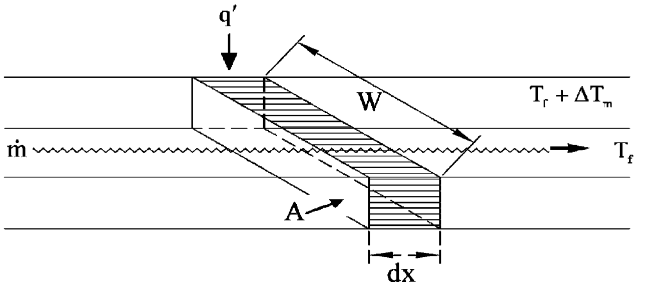

Fig. 3. Forced convection heat transfer inside duct of a solar air heater.

Focusing on a slice of thickness dx as a system, the rate of entropy generation is given by the second law of thermodynamics:

$$\mathrm{d}\dot{S}_{\mathrm{gen}} = \dot{m}\,\mathrm{d}s - \frac{q'\,\mathrm{d}x}{T_{\mathrm{f}} + \Delta T_{\mathrm{m}}}. \tag{2}$$

The first law of thermodynamics is applied to the same system as

$$\dot{m}\,\mathrm{d}h = q'\,\mathrm{d}x. \tag{3}$$

In addition, for any pure substance we can write

$$\frac{\mathrm{d}h}{\mathrm{d}x} = T_{\mathrm{f}}\frac{\mathrm{d}s}{\mathrm{d}x} + \frac{1}{\rho}\frac{\mathrm{d}P}{\mathrm{d}x}. \tag{4}$$

Substituting ds given by Eq. (2) and dh given by Eq. (3) into Eq. (4) yields the entropy generation rate per unit duct length as

$$\dot{S}'_{\mathrm{gen}} = \frac{q'\,\Delta T_{\mathrm{m}}}{T_{\mathrm{f}}^2(1+\tau)} + \frac{\dot{m}}{\rho T_{\mathrm{f}}}\left(-\frac{\mathrm{d}P}{\mathrm{d}x}\right), \tag{5}$$

where $\dot{S}'_{\mathrm{gen}} = \mathrm{d}\dot{S}_{\mathrm{gen}}/\mathrm{d}x$.

In solar air heater dimensionless temperature difference τ $(= \Delta T_{\mathrm{m}}/T_{\mathrm{f}})$ is negligible compared to unity, we have the simpler form:

$$\dot{S}'_{\mathrm{gen}} = \frac{q'\Delta T_{\mathrm{m}}}{T_{\mathrm{f}}^2} + \frac{\dot{m}}{\rho T_{\mathrm{f}}}\left(-\frac{\mathrm{d}P}{\mathrm{d}x}\right) = S'_{\Delta T} + S'_{\Delta P}. \tag{6}$$

The first term, $S'_{\Delta T}$ represents the irreversibility due to heat transfer across the wall–fluid temperature difference and the second term, $S'_{\Delta P}$ is the irreversibility caused by fluid friction.

The relative importance of the two irreversibility mechanism is described by the *irreversibility distribution ratio*, ψ [6] which is defined as

$$\psi = \frac{\text{fluid friction irreversibility}}{\text{heat transfer irreversibility}} = \frac{\dot{S}'_{\mathrm{gen},\Delta P}}{\dot{S}'_{\mathrm{gen},\Delta T}}. \tag{7}$$

Therefore Eq. (6) can be written as $\dot{S}'_{\mathrm{gen}} = (1+\psi)S'_{\Delta T}$. Eq. (6) can now be related to average heat transfer and fluid-friction information for the solar air heater duct geometry. We recall that in heat transfer, the relationship between the heat transfer rate, q' and wall–bulk fluid temperature difference can be expressed in the form of Stanton number:

$$St = \frac{q'/W\Delta T_{\mathrm{m}}}{C_p G}, \tag{8}$$

where $G\ (= \dot{m}/WH)$ is the mass velocity. The fluid friction characteristics of a duct are usually reported in the form of friction factor as

$$f = \frac{\rho D}{2G^2}\left(-\frac{\mathrm{d}P}{\mathrm{d}x}\right). \tag{9}$$

The friction factor depends on the Reynolds number and other geometric parameters of the duct. In order to illustrate the dependence of $\dot{S}'_{\mathrm{gen}}$ on Stanton number and friction factor information, combining Eqs. (8) and (9) with Eq. (6) yields

$$\dot{S}'_{\mathrm{gen}} = \frac{1}{St}\frac{q'}{T_{\mathrm{f}}^2}\frac{1}{W\,C_p\,G} + f\frac{2V^2\dot{m}}{DT_{\mathrm{f}}} \tag{10}$$

and irreversibility distribution ratio can be put in the simpler non-dimensional form as

$$\psi = 2\left(\frac{f/2}{St}\right)\left(1+\frac{H}{W}\right)\left(\frac{V^2}{C_p\,T_{\mathrm{f}}}\right)\left(\frac{T_{\mathrm{f}}}{\Delta T_{\mathrm{m}}}\right)^2, \tag{11}$$

where V is the fluid velocity in the duct.

The impact of an augmentation technique on the irreversibility of a known solar air heater duct can be evaluated directly by calculating the entropy generation rate in the augmented passage, $\dot{S}'_{\mathrm{gen,a}}$ (suffix 'a' for augmented surface and 's' for smooth surface) and comparing it with the entropy generation rate in the conventional solar air heater, $\dot{S}'_{\mathrm{gen,s}}$. To quantize the thermodynamic impact of the augmentation technique, Bejan [6] has defined the augmentation entropy generation number, as $N_{\mathrm{a}} = \dot{S}'_{\mathrm{gen,a}}/\dot{S}'_{\mathrm{gen,s}}$.

Augmentation techniques yielding values of N_{a} less than unity are thermodynamically advantageous since in addition to enhancing heat transfer they reduce the irreversibility of the system. In case of a solar air heater where the temperature rise parameter are specified and for the purpose of comparison there is no harm to consider the insolation is constant. Temperature rise parameter, $(T_{\mathrm{o}} - T_{\mathrm{i}})/I$ is specified, T_{i} and I are taken as constant. Therefore T_{o} and $T_{\mathrm{f}}\ [= (T_{\mathrm{i}} + T_{\mathrm{o}})/2]$ are constant. Under this consideration the ratio of useful heat gain, $Q_u\{= \dot{m}C_p(T_{\mathrm{o}} - T_{\mathrm{i}})\}$ for the augmented duct to the conventional duct can be written as

$$\frac{Q_{\mathrm{u,a}}}{Q_{\mathrm{u,s}}} = \frac{q'_{\mathrm{a}}}{q'_{\mathrm{s}}} = \frac{\dot{m}_{\mathrm{a}}}{\dot{m}_{\mathrm{s}}} = \frac{Re_{\mathrm{a}}}{Re_{\mathrm{s}}}$$

and the ratio of Stanton number $\dfrac{St_{\mathrm{a}}}{St_{\mathrm{s}}} = \dfrac{\Delta T_{\mathrm{m,s}}}{\Delta T_{\mathrm{m,a}}}$.

Then the augmentation entropy generation number can be expressed as

$$N_{\mathrm{a}} = \frac{St_{\mathrm{s}}}{St_{\mathrm{a}}}\frac{(1+\psi_{\mathrm{a}})}{(1+\psi_{\mathrm{s}})}\frac{Re_{\mathrm{a}}}{Re_{\mathrm{s}}}. \tag{12}$$

Rearranging it can be written as

$$N_{\mathrm{a}}=\frac{Re_{\mathrm{a}}}{Re_{\mathrm{s}}}\left(\frac{\psi_{\mathrm{s}}}{1+\psi_{\mathrm{s}}}\right)\left[\frac{f_{\mathrm{a}}}{f_{\mathrm{s}}}\left(\frac{Re_{\mathrm{a}}}{Re_{\mathrm{s}}}\right)^{2}-\frac{St_{\mathrm{s}}}{St_{\mathrm{a}}}\right]+\frac{Re_{\mathrm{a}}}{Re_{\mathrm{s}}}\frac{St_{\mathrm{s}}}{St_{\mathrm{a}}}. \tag{13}$$

In general, N_{a} is a function of the Stanton number ratio and the friction factor ratio of roughened absorber surface to the smooth conventional solar air heater. If the solar air heater duct is known, the irreversibility distribution ratio for the smooth duct ψ_{s} can be calculated easily; its numerical value describes the thermodynamic mode in which the passage is meant to function:

$$\psi_{\mathrm{s}}=2\left(\frac{f_{\mathrm{s}}/2}{St_{\mathrm{s}}}\right)\left(1+\frac{H}{W}\right)\left(\frac{V^{2}}{C_{p}T_{\mathrm{f}}}\right)_{\mathrm{s}}\left(\frac{T_{\mathrm{f}}}{\Delta T_{\mathrm{m}}}\right)_{\mathrm{s}}^{2}. \tag{14}$$

For a fixed temperature rise parameter and roughness parameters there exists a critical irreversibility distribution ratio, where $N_{\mathrm{a}}=1$, i.e., where the augmentation technique has absolutely no effect on irreversibility. From an engineering standpoint, it is important to know priori to the roughening an absorber plate of a solar air heater, under what conditions the wall roughening technique leads to a reduction in entropy generation. If in a certain design, the actual ψ_{s} is lower than the critical ψ_{s} value, the use of artificial roughness will reduce the rate of entropy generation in the duct passage. The critical irreversibility distribution ratio ($\psi_{\mathrm{s,c}}$) can be obtained setting $N_{\mathrm{a}}=1$ in Eq. (13) as

$$\psi_{\mathrm{s,c}}=\frac{1-\frac{St_{\mathrm{s}}}{St_{\mathrm{a}}}\left(\frac{Re_{\mathrm{a}}}{Re_{\mathrm{s}}}\right)}{\frac{f_{\mathrm{a}}}{f_{\mathrm{s}}}\left(\frac{Re_{\mathrm{a}}}{Re_{\mathrm{s}}}\right)^{3}-1}. \tag{15}$$

3. Method of computation

The thermal behavior of artificially roughened solar air heater is similar to that of usual flat plate conventional air heater; therefore, the usual procedures of calculating the absorbed irradiation and the heat losses can be used. The most important assumptions and simplifications which have been used are:

- steady-state conditions;
- heat conduction in flow direction neglected;
- edge effects neglected; constant air flow throughout the collector;
- sky treated as black body with a temperature equal to the ambient temperature.

Experimental investigations to determine Nusselt number and friction factor depending on the geometrical parameters have been done by the authors; these correlations are used here for the numerical analysis. As discussed earlier, the thermal performance of a solar air heater can be predicted on the basis of detailed consideration of heat transfer processes in the system. The performance parameters, namely overall heat loss coefficient, heat removal factor and other relevant factors can then be evaluated. For this purpose a step by step procedure has to be followed. The salient features of the procedure are discussed below. The objective of this work is to present a methodology for optimal design of solar air heater. Results need to be presented in terms of two basic design parameters namely; Temperature rise parameter, $\Delta T/I$ (ratio of air temperature rise across the duct, $(T_o - T_i)$ to the average intensity of insolation and insolation (I). For a given collector the calculation starts with considering fixed value for these two variable operating parameters and proceeds with the calculation of the other parameters. Step by step procedure of calculation is given below. A computer program is developed in MATLAB for this purpose.

A set of system roughness parameter namely relative roughness height (e/D_h), relative roughness pitch (P/e), relative groove position (g/P) and Chamfer angle (ϕ) is selected for which the calculation is to be performed. Fixed system parameters, e.g., Thickness of insulation, t_i, Thermal conductivity of insulation, k_i, Transmittance–absorptance product, $(\tau\alpha)$, emissivity of the absorber plate, ε_p and emissivity of the glass cover, ε_c and fixed operating parameters, e.g., velocity of the air, V_w is considered as 1 m/s, an approximate atmospheric temperature, T_a is considered as 300 K, the temperature rise of air across the duct and the outlet temperature is calculated as; $T_o = \Delta T/I + T_i$.

The numerical calculations are carried out by employing the values as follows: $\tau\alpha = 0.9$, $\varepsilon_p = 0.8$, $t_g = 0.003\,\text{m}$, $k_g = 078\,\text{W/mK}$, $\varepsilon_c = 0.88$, $V = 1\,\text{m/s}$, $T_{sun} = 5762\,\text{K}$, $H = 0.03\,\text{m}$, $L = 1.5\,\text{m}$, $W = 1\,\text{m}$.

It is assumed that the solar radiation intensity is constant of $800\,\text{W/m}^2$. Thermo physical properties of air employed in the calculation were picked up from available tables in [7] corresponding to mean bulk air temperature.

Approximate initial plate temperature is assumed, T_p, using the assumed value of plate temperature, T_p, the value of the top loss coefficient, U_t is computed using the relation given in Mullick and Samdarshi [8], the back loss coefficient U_b, is expressed as, $U_b = k/\delta_b$, the edge loss coefficient, based on the collector area A_p is calculated as

$$U_e = \frac{(UA)_{edge}}{A_p} = \frac{(L + W)L_3}{LW\delta_i}k_i.$$

Consequently, $U_l = U_t + U_b + U_e$ and useful heat gain rate is calculated as: $Q_u = [I(\tau\alpha) - U_L - (T_p - T_a)]A_p$. Mass flow rate and Reynolds number of flow of air in the duct is computed as: $\dot{m} = Q_{u1}/C_p\Delta T$; $Re = G_o D_h/\mu$ where $G_o = \dot{m}/WH$ is the mass velocity of air through the collector. The heat transfer coefficient is calculated $\left(h = Nuk/D_h\right)$ using the Nusselt number correlation obtained from the experimental observation as

$$\begin{aligned} Nu = {} & 0.0028Re^{0.93}\left(\frac{e}{D_h}\right)^{0.528}\left(\frac{P}{e}\right)^{2.17}\left(\frac{g}{P}\right)^{-1.054} \\ & \times\phi^{0.77}\left[\exp\left(-0.138(\ln\,\phi)^2\right)\right] \\ & \times\left[\exp\left\{-0.57\left(\ln\frac{P}{e}\right)^2\right\}\right] \\ & \times\left[\exp\left\{-0.649\left(\ln\frac{g}{P}\right)^2\right\}\right]. \end{aligned}$$

The plate efficiency factor is then computed as, $F' = h/(h + U_L)$ and the heat removal factor, F_o based on outlet temperature is calculated as

$$F_o = \frac{\dot{m}C_p}{A_p U_l}\left[1 - \exp\left\{-\frac{F' U_l A_p}{\dot{m}C_p}\right\}\right].$$

Now useful heat gain is calculated based on heat removal factor, $Q_{u1} = A_p F_o[I(\tau\alpha) - U_l(T_o - T_i)]$. The value of Q_u and Q_{u1} are compared; if the difference is more than the 0.1% of Q_u, then the new value of plate temperature is calculated as, $(T_p)_n = T_a + [(I(\tau\alpha) - Q_u/A_p)/U_L]$.

Using this new value of plate temperature, the above steps are repeated until the convergence is obtained. The friction factor value is then calculated from the correlation obtained from experimental observation and reproduced below as

$$f = 0.00276\,Re^{-0.1279}\left(\frac{e}{D_h}\right)^{0.3632}\left(\frac{P}{e}\right)^{4.255}\left(\frac{g}{P}\right)^{-0.976} \times \exp[0.00575\phi]\exp\left[-1.066\left(\ln\frac{P}{e}\right)^2\right] \times \exp\left[-0.583\left(\ln\frac{g}{P}\right)^2\right].$$

Now pressure drop across the duct can be calculated from $(\Delta P)_d = 4fL\rho V^2/2D_h$ and the mechanical power required to drive the air through the duct is calculated from $P_m = m(\Delta P)_d/\rho$. The *augmentation entropy generation number* is then calculated using Eq. (13) and the critical irreversibility distribution ratio can be obtained using Eq. (15). Next set of values of temperature rise parameter and insolation is selected and the above steps are repeated to cover the possible range of temperature rise parameter and insolation. Next set of roughness parameter, e.g. relative roughness height (e/D_h), relative roughness pitch (P/e), relative groove position (g/P), Chamfer angle (ϕ) is selected and the computation are repeated to cover the entire range of roughness parameters.

4. Results and discussion

Fig. 4 shows the augmentation entropy generation number, N_a as a function of temperature rise parameter and relative roughness height. It is evident that the ability of the chamfered rib–groove roughened absorber plate to reduce irreversibility depends on the thermo-fluid operating regime, ψ_s and temperature rise parameter. The entropy generation rate decreases sharply with increase in temperature rise parameter reaches its minima for temperature rise parameter of about 0.007 $\mathrm{K/m^2\,W}$ and increases steadily with further increase in temperature rise parameter. The entropy generation decreases with the increase in relative roughness height. Fig. 5 depicts the effect of relative roughness pitch on the augmentation entropy generation number, N_a. For the temperature rise parameter higher than 0.006 $\mathrm{K/m^2\,W}$ relative roughness pitches of 6 have the best performance while the relative roughness pitch of 10 is the lowest. For the temperature rise parameter lower than 0.006 $\mathrm{K/m^2\,W}$ relative roughness pitches of 4.5 have the best performance. Fig. 6 shows the effect of relative groove position on augmentation entropy generation number, N_a. It can be seen that the relative groove position of 0.4 has the best performance for the temperature rise parameter of higher than 0.004 $\mathrm{K/m^2\,W}$ and 0.3 has the lowest. For the temperature rise parameter lower than 0.004 $\mathrm{K/m^2\,W}$ the trend is reversed. Fig. 7 shows the effect of chamfering of the rib top on augmentation entropy generation number, N_a with variation in temperature rise parameter. It can be seen that due to change in chamfer angle from 5° to 18° has a remarkable effect.

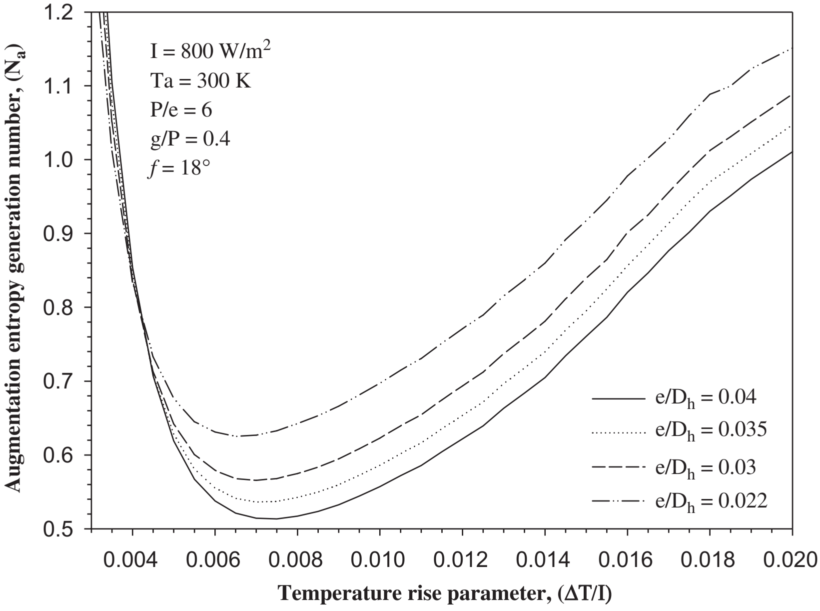

Fig. 4. The effect of relative roughness height on augmentation entropy generation number.

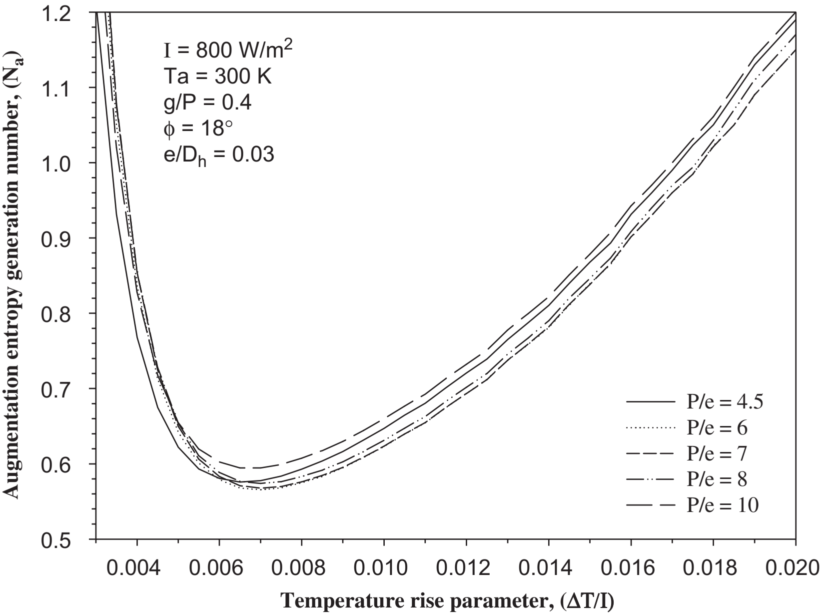

Fig. 5. The effect of relative roughness pitch on augmentation entropy generation number.

In Figs. 8–11 the marginal curves are plotted for $\psi_{s,c}$ resulting from setting $N_a = 1$ in Eq. (15). Below each curve, roughening the wall decreases the irreversibility rate. If in a certain design, the actual $\psi_{s,c}$ exceeds the critical ψ_s value the use of chamfer rib–groove

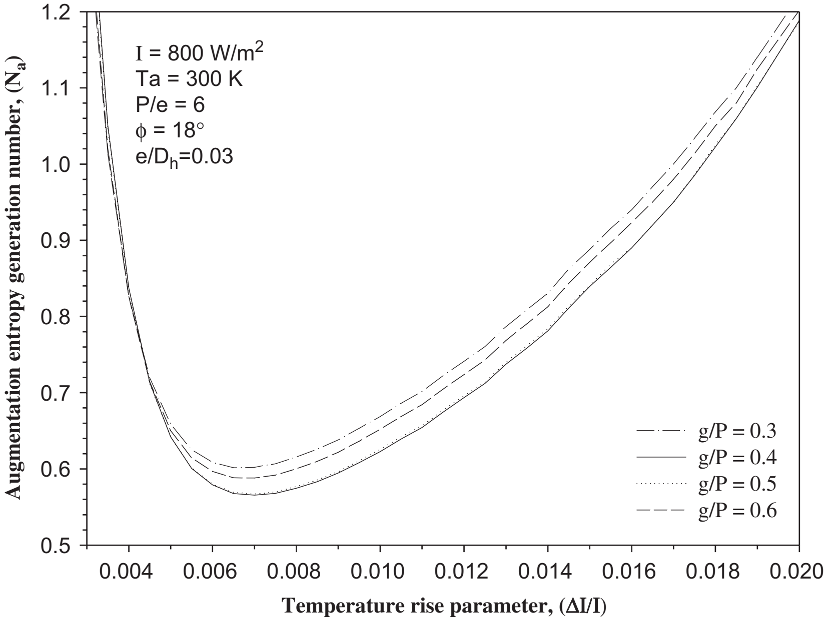

Fig. 6. The effect of relative groove position on augmentation entropy generation number.

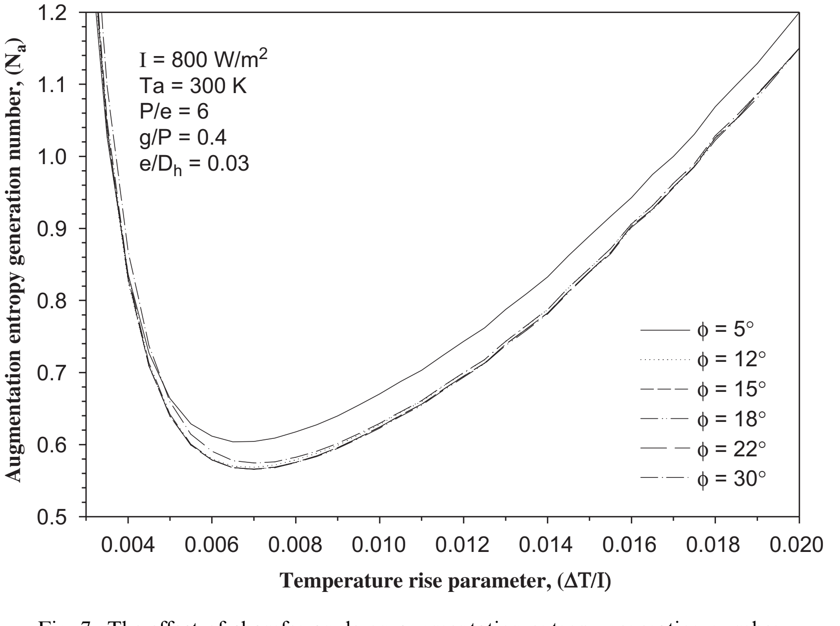

Fig. 7. The effect of chamfer angle on augmentation entropy generation number.

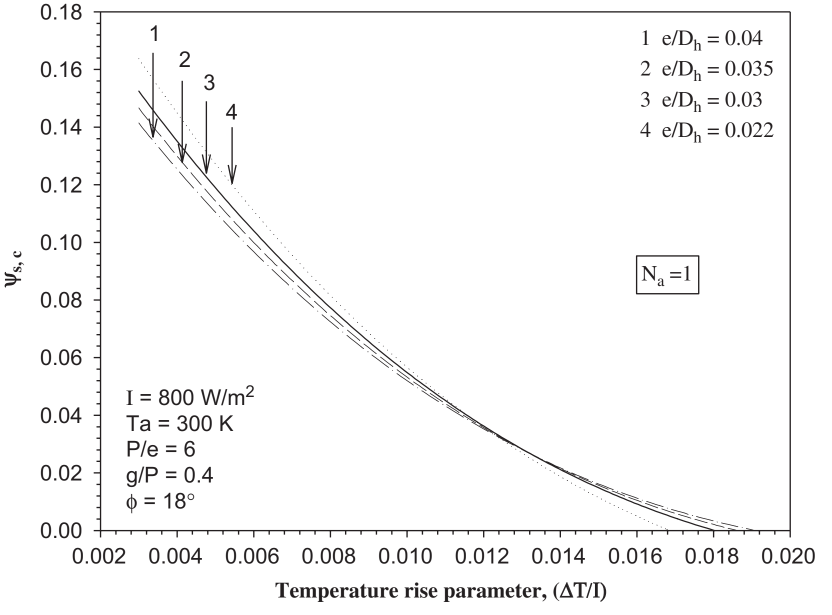

Fig. 8. The effect of relative roughness height on critical irreversibility distribution ratio.

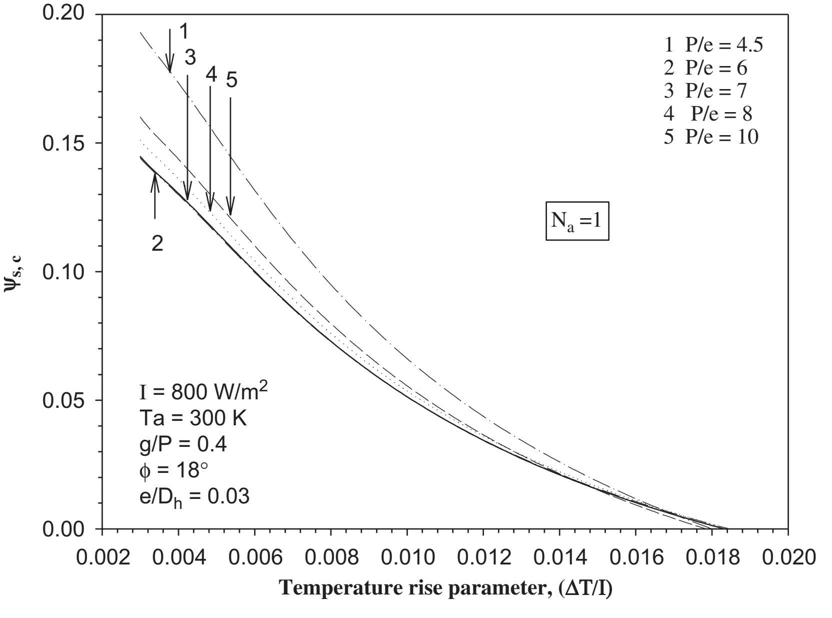

Fig. 9. The effect of relative roughness pitch on critical irreversibility distribution ratio.

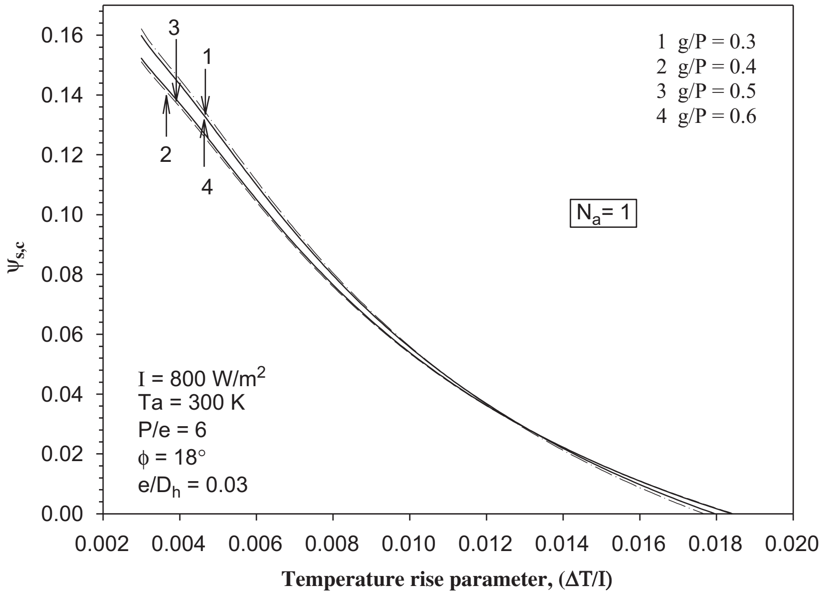

Fig. 10. The effect of relative groove position on critical irreversibility distribution ratio.

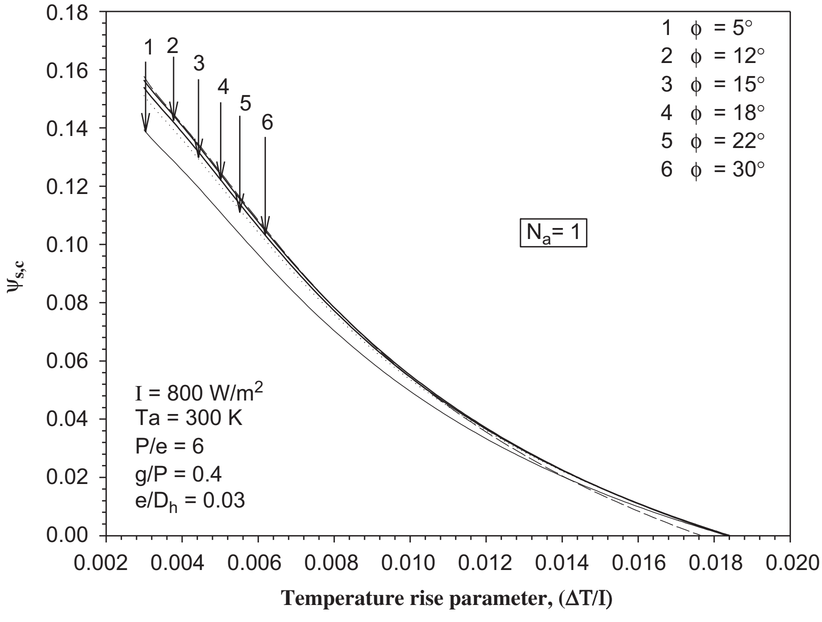

Fig. 11. The effect of chamfer angle on critical irreversibility distribution ratio.

compound roughness will reduce the rate of entropy generation in the solar air heater duct. This point of view is related to the one used to construct these plots where the critical $\psi_{s,c}$ mark the boundary of the domain in which heat transfer enhancement is thermodynamically acceptable.

5. Conclusions

This study presents the mathematical model for predicting the entropy generation of a solar air heater having chamfered rib–groove roughened absorber plate. Effect of the roughness parameter on the entropy generation is considered. It was found that the entropy generation decreases with increase in relative roughness height. The set of relative roughness pitch of 6, relative groove position 0.4 and chamfer angle 18° shows the minimum rise in entropy generation.

References

[1] Karwa R, Solanki SC, Saini JS. Heat transfer coefficient and friction factor correlations for the transient flow regime in rib-roughened rectangular ducts. Int J Heat Mass Transfer 1999;42:1597–615.
[2] Liou TM, Hwang JJ. Turbulent heat transfer augmentation and friction in periodic fully developed channel flows. ASME/J Heat Transfer 1992;114:56–64.
[3] Ravigururajan TS, Bergles AE. Development and verification of general correlations for pressure drop and heat transfer in single-phase turbulent flow in enhanced tubes. Exp Therm Fluid Sci 1996;13:55–70.
[4] Williams F, Pirie MAM, Warburton C. Heat transfer from surfaces roughened by ribs. ASME/Augmentation of Heat Transfer, New York 1970;36–43.
[5] Zhang YM, Gu WZ, Han JC. Heat transfer and friction in rectangular channel with ribbed or ribbed-grooved walls. ASME/J Heat Transfer 1994;116:58–65.
[6] Bejan A. Entropy generation through heat and fluid flow. New York: Wiley-Interscience Publication; 1982.
[7] Duffie JA, Beckman WA. Solar engineering of thermal processes. New York: Wiley; 1980.
[8] Mullick SC, Samdarshi SK. An improved technique for computing the top heat loss factor of a flat plate collector with a single glazing. ASME/J Sol Energy Eng 1988;110:262–7.